

# Global Evolutionary Algorithms in the Design of Electromagnetic Band Gap Structures with Suppressed Surface Waves Propagation

Peter KOVÁCS, Zbyněk RAIDA

Dept. of Radio Electronics, Brno University of Technology, Purkyňova 118, 612 00 Brno, Czech Republic

xkovac04@stud.feec.vutbr.cz, raida@feec.vutbr.cz

**Abstract.** *The paper is focused on the automated design and optimization of electromagnetic band gap structures suppressing the propagation of surface waves. For the optimization, we use different global evolutionary algorithms like the genetic algorithm with the single-point crossover (GAs) and the multi-point (GAm) one, the differential evolution (DE) and particle swarm optimization (PSO). The algorithms are mutually compared in terms of convergence velocity and accuracy. The developed technique is universal (applicable for any unit cell geometry). The method is based on the dispersion diagram calculation in CST Microwave Studio (CST MWS) and optimization in Matlab. A design example of a mushroom structure with simultaneous electromagnetic band gap properties (EBG) and the artificial magnetic conductor ones (AMC) in the required frequency band is presented.*

## Keywords

Electromagnetic band gap (EBG), optimization, genetic algorithm (GA), differential evolution (DE), particle swarm optimization (PSO), CST Microwave Studio (CST MWS), Matlab.

## 1. Introduction

Electromagnetic band gap (EBG) structures became widely used in microwave- and radio engineering in the last decades of the 20<sup>th</sup> century for the implementation of filters, antenna substrates with suppressed propagation of surface waves, superstrates and artificial magnetic conductors (AMC). The automated design and optimization by global evolutionary algorithms (primarily by variants of genetic algorithms) was successfully implemented in case of superstrates [1] and AMC surfaces [2]. However, the utilization of these methods for the synthesis of special substrates with the suppressed propagation of surface waves in a given frequency band has not been published in the open literature yet. Moreover, the design of such structures is rather complicated due to

the uncertain dependence of EBG properties on parameters of the unit cell. Without a proper approach, the design of such a structure is based on trial-and-error.

In this paper, a universal technique for the automated design and optimization of EBG structures with suppressed propagation of surface waves is presented. The method is based on the calculation of the dispersion diagram in the full-wave electromagnetic solver CST Microwave Studio (CST MWS), and on the optimization by a global evolutionary algorithm implemented in Matlab. Four types of algorithms were developed to compare their convergence velocity and accuracy: the binary coded genetic algorithm with the single-point crossover (GAs) and the multi-point one (GAm), the differential evolution (DE) in the basic variant and the particle swarm optimization (PSO).

In the last section, an example of the design of a mushroom structure with simultaneous EBG and AMC properties in the required frequency interval is presented. The results obtained by CST MWS are compared to the results calculated in Ansoft HFSS.

## 2. Global Evolutionary Algorithms in the Design of EBG Structures

The design of an EBG structure begins with the dispersion analysis. The dispersion analysis is based on the unit cell modelling and the application of periodic boundary conditions in the appropriate directions. The computed dispersion diagram, which is a graphical representation of the dependence of the propagation constant on frequency, gives us the accurate position of stop bands in the frequency spectrum. Because of the slow-wave behavior of surface waves, dispersion curves are calculated in the region under the light line only. The EBG unit cell models in CST MWS and Ansoft HFSS for the surface waves dispersion diagram computation are depicted in Fig. 1. Credibility of the results obtained by two different software tools (CST MWS, Ansoft HFSS) was discussed in [3] and [4]. The developed GAs, GAm, DE and PSO algorithms were tested on a simple planar EBG

unit cell depicted in Fig. 2. For the optimization, the period  $D$  and the size of the square patch  $P$  were selected as state variables. The relative permittivity  $\epsilon_r$  and height  $h$  of the dielectric substrate are considered to be constant and equal to 6.15, and 1.575 mm, respectively. The required center frequency of the band gap of the TE surface wave (occurring between the second and the third dispersion curve) is  $f_c = 5.5$  GHz. In all the cases, the fitness (or objective) function  $F$  is formulated as a two-criterion function with respect to both the band gap position and the maximum bandwidth. The function is going to be minimized

$$F = \left( \frac{f_{BG\_max} + f_{BG\_min}}{2} - f_c \right)^2 - \left( \frac{f_{BG\_max} - f_{BG\_min}}{f_c} \right). \quad (1)$$

In (1),  $f_{BG\_min}$  is the lower limit and  $f_{BG\_max}$  is the upper limit of the band gap.

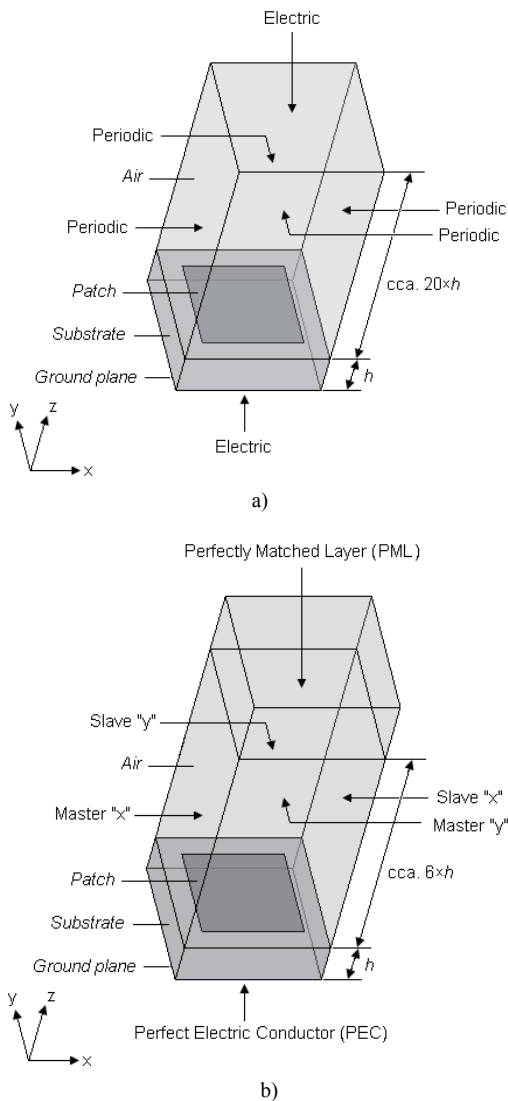


Fig. 1. Unit cell setup for dispersion diagram computation: CST MWS (a), Ansoft HFSS (b).

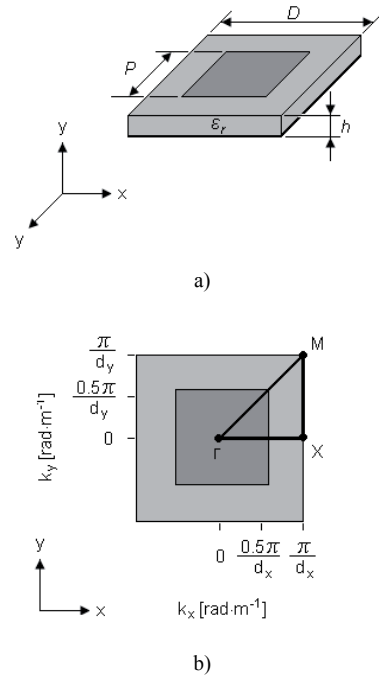


Fig. 2. The EBG unit cell under consideration (a), the irreducible Brillouin zone for dispersion diagram computation (b). Parameters  $k_x, k_y$  are the  $x$  and  $y$  components of the wave vector  $\mathbf{k}$ .

### 2.1 Binary Coded Genetic Algorithm with Single-Point and Multi-Point Crossover

Genetic algorithm optimizers are robust, stochastic search methods, modeled on the principles and concepts of the natural selection and evolution [5]. The flowchart of the proposed genetic algorithms is depicted in Fig. 3.

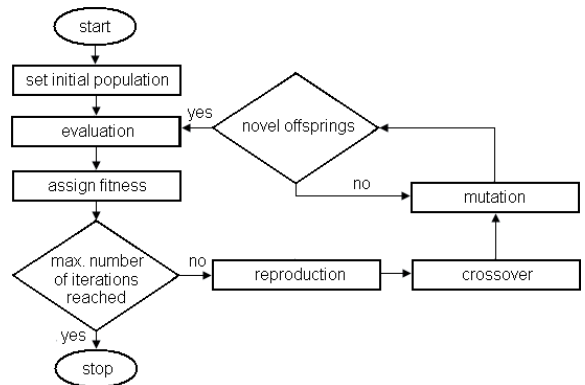
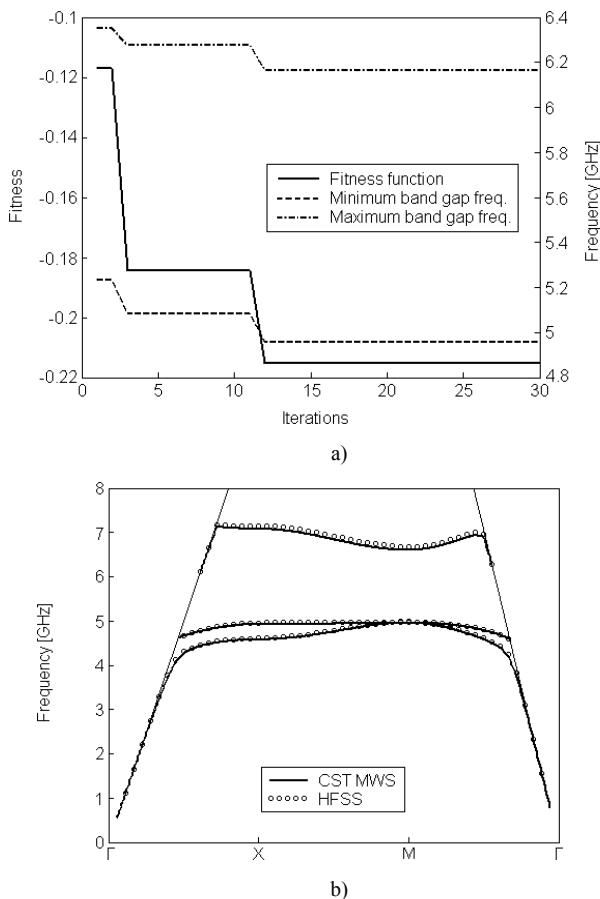


Fig. 3. Flowchart of the working principle of the proposed genetic algorithms.

The state variables of the optimized structure are binary encoded and put into a binary array (gene). Each individual is represented by 10 bits: 5 bits are used for the period  $D$  and 5 bits for the patch size  $P$ . The minimum and the maximum value of the period are set to 8.0 mm and 23.5 mm, respectively. The size of the patch is defined



**Fig. 4.** Genetic algorithm with single-point crossover: evaluation of the fitness function and of the lower / upper band gap frequency during 30 iterations (a), dispersion diagram of the best individual (b).

within the range of  $\langle 0.50 D, 0.95 D \rangle$ . The initial population consists of 12 random individuals. In order to delete the individuals with the highest values of the fitness function, population decimation is applied in the process of reproduction: the 6 worst individuals are erased and the 6 best individuals are copied without any change into the next generation (elitism). The remaining 6 new ones are created by the crossover and mutation (a random bit inverse). The probability of the crossover is 100 % and the probability of the mutation is set to 6 %. Because of a relatively small resolution (0.5 mm for the period), offspring are controlled in terms of their originality – the process of mutation is repeated for all the newly created individuals that were already considered in previous iterations.

In this work, two variants of the genetic algorithm were realized: the first one uses the single-point crossover (genes of parameters  $D$  and  $P$  are not crossed separately), and the second one uses the multi-point crossover (genes of parameters  $D$  and  $P$  are crossed separately).

In Fig. 4 and Fig. 5, results of the optimization process obtained by the GA with the single-point crossover and the GA with the multi-point crossover are depicted. Parameters of the best individuals for all the optimization methods considered in the paper are listed in Tab. 1.

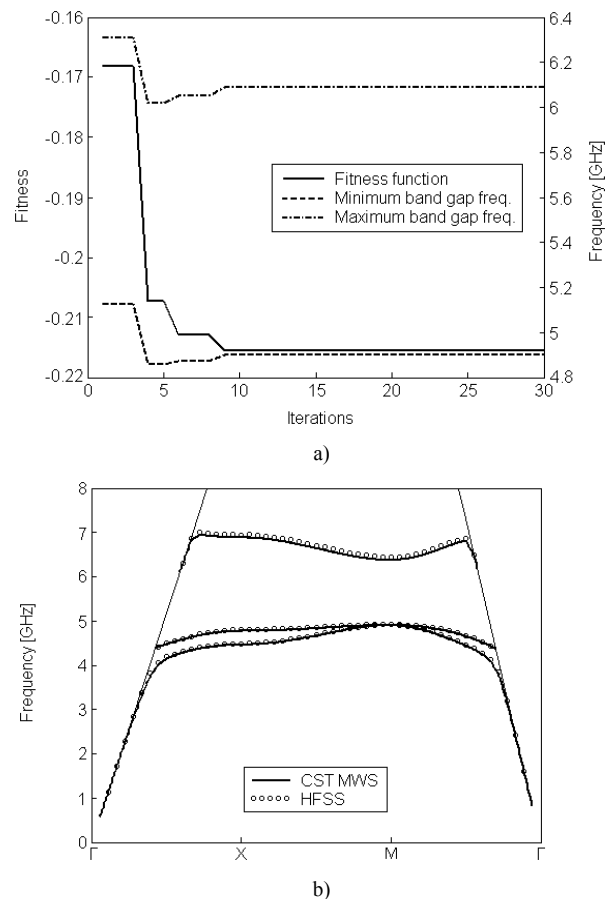


**Fig. 5.** Genetic algorithm with multi-point crossover: evaluation of the fitness function and of the lower / upper band gap frequency during 30 iterations (a), dispersion diagram of the best individual (b).

## 2.2 Differential Evolution

A differential evolution algorithm in the basic variant is the third method proposed in this work for the EBG unit cell design. The crucial idea behind DE is a scheme for generating trial parameter vectors, see Fig. 6 [6], [7]. Individuals for the mutant population are created by adding a weighted difference between two population vectors to a third vector. After crossover and parameter control, values of the objective functions of the trial and target vector are compared: the individual with the higher value of the objective function is erased.

Similarly to the GA, the initial population of the DE algorithm consists of 12 individuals. However, the period  $D$  and the patch size  $P$  can change arbitrarily in the defined intervals ( $D \in \langle 8.0 \text{ mm}, 23.5 \text{ mm} \rangle$ ,  $P \in \langle 0.50 D, 0.95 D \rangle$ ) since  $D$  and  $P$  are real-valued parameters. A parameter of the trial vector, which overflows the defined range during the differential mutation, is replaced by an allowed random value. Moreover, the DE algorithm creates 12 new individuals in each iteration cycle in comparison to 6 new individuals in case of the GA. Both the value of the mutation scale factor  $F$  and the value of the crossover constant  $C$  are set to 0.5. Fig. 7 shows a design example of the investigated EBG by the developed DE code.

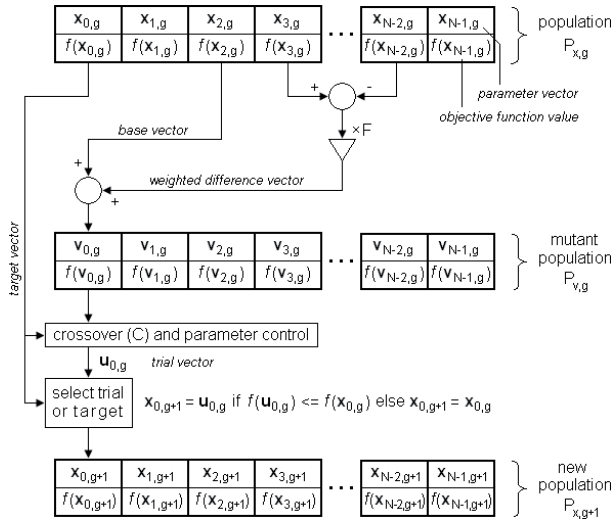


Fig. 6. Working principle of the differential evolution algorithm.

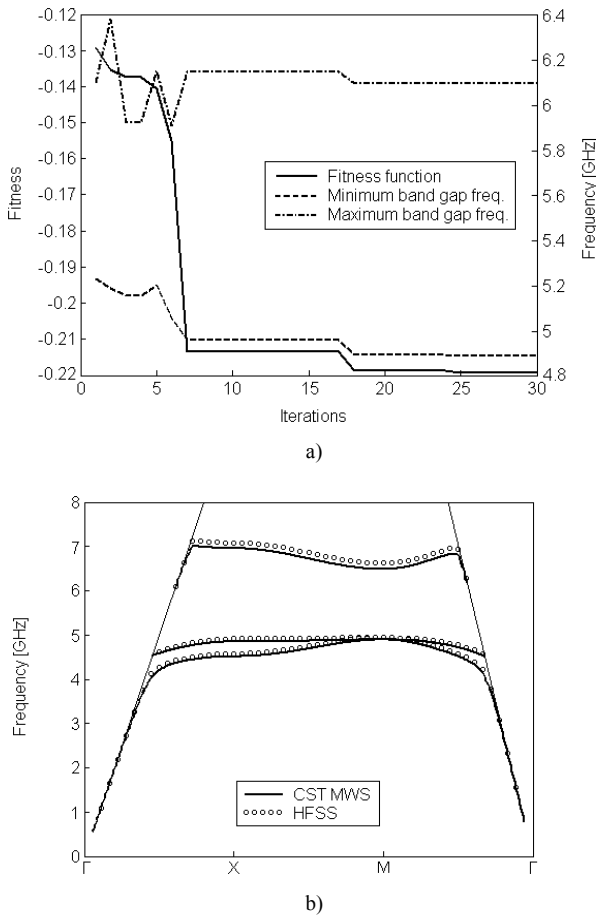


Fig. 7. Differential evolution: evaluation of the fitness function and of the lower / upper band gap frequency during 30 iterations (a), dispersion diagram of the best individual (b).

### 2.3 Particle Swarm Optimization

The PSO algorithm is the fourth method tested for the design and optimization of EBG. PSO is based on the movement and the intelligence of swarms [8]. A swarm of

bees is aimed to find the best flowers in a feasible space. The bees are described by their coordinates, their velocity of movement and their value of the objective function. Each bee remembers the position of the lowest value of the fitness function reached during its fly (the personal best position). Moreover, each bee also knows the position of the lowest minim revealed by the swarm together (the global best position). The velocity vector  $\mathbf{v}$  (the direction and the speed of flight) of the bee to the area of the best flowers in the  $(n+1)$  iteration step can be expressed by the equation [8]

$$\mathbf{v}_{n+1} = K \cdot (\mathbf{v}_n + \varphi_1 \cdot r_1 \cdot (\mathbf{p}_{best} - \mathbf{x}_n) + \varphi_2 \cdot r_2 \cdot (\mathbf{g}_{best} - \mathbf{x}_n)) \quad (2)$$

where  $K$ ,  $\varphi_1$  is the personal best scaling factor and  $\varphi_2$  is the global best scaling factor,  $r_1$  and  $r_2$  are random numbers ranging from 0 to 1,  $\mathbf{p}_{best}$  is the position of the personal best position,  $\mathbf{g}_{best}$  is the location of the global best position and  $\mathbf{x}_n$  is the current position of the bee (in the  $n$ -th iteration step). For the optimization, values of constants were set to  $K = 0.729$ ,  $\varphi_1 = 2.8$ ,  $\varphi_2 = 1.3$  [8]. Once the velocity vector of a bee is known, its new position can be calculated [8]

$$\mathbf{x}_{n+1} = \mathbf{x}_n + \Delta t \cdot \mathbf{v}_{n+1} \quad (3)$$

In (3),  $\Delta t$  is the time period the bee flies by the velocity  $\mathbf{v}_{n+1}$  (in our case,  $\Delta t$  was set to 1 second). In order to keep the bees in the feasible space, the “absorbing wall” boundary condition was used: if the bee reaches the border, the magnitude of the normal component of the velocity vector is set to zero.

Similarly to the previous cases, the population consists of 12 individuals, and parameters of the unit cell  $D$  and  $P$  are defined in intervals of  $D \in \langle 8.0 \text{ mm}, 23.5 \text{ mm} \rangle$  and  $P \in \langle 0.50D, 0.95D \rangle$ , respectively. In Fig. 8, an example of the planar EBG unit cell designed by PSO algorithm is shown.

### 2.4 Comparison of the Methods

In the previous sections, ability of different global evolutionary algorithms was tested in the design of EBGs suppressing the propagation of surface waves. Attention was turned to finding the optimum values of parameters  $D$  and  $P$  of the unit cell for the given permittivity  $\epsilon_r = 6.15$  and thickness  $h = 1.575 \text{ mm}$  of the dielectric substrate (see Fig. 2.a). Results depicted in Figures 4, 5, 7 and 8 are summarized in Tab. 1.

The solutions produced by the considered methods are very similar. In all the cases, the optimum values of  $D$  and  $P$  for the central frequency  $f_c = 5.5 \text{ GHz}$  and the maximum bandwidth are about 15 mm and 12 mm, respectively. The achieved relative bandwidth BW (related to  $f_c = 5.5 \text{ GHz}$ ) is approximately 21%.

Let us investigate the effectiveness of the considered techniques in term of the required computational time. The dispersion relation of the planar square EBG unit cell was calculated with the phase step 20 degrees for the first three

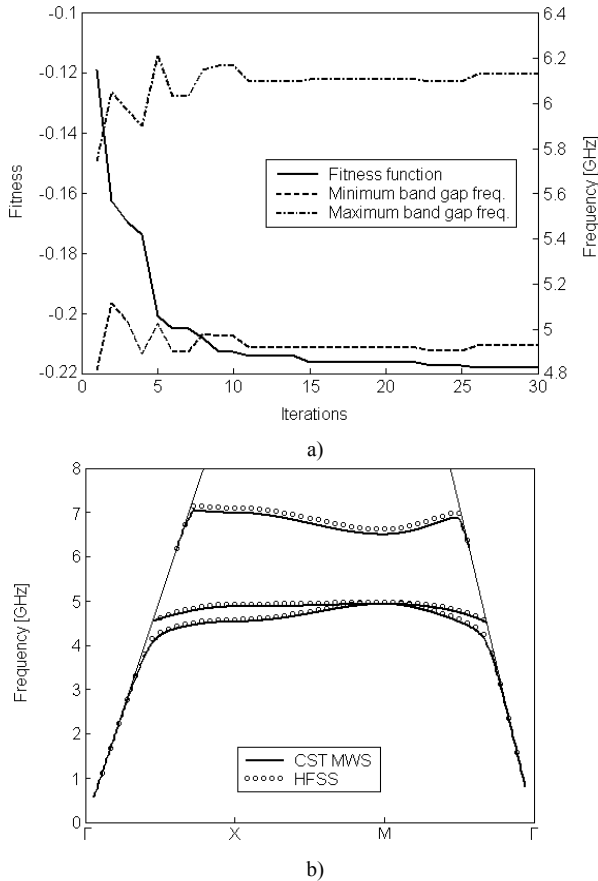


**Fig. 8.** Particle swarm optimization: evaluation of the fitness function and of the lower / upper band gap frequency during 30 iterations (a), dispersion diagram of the best individual (b).

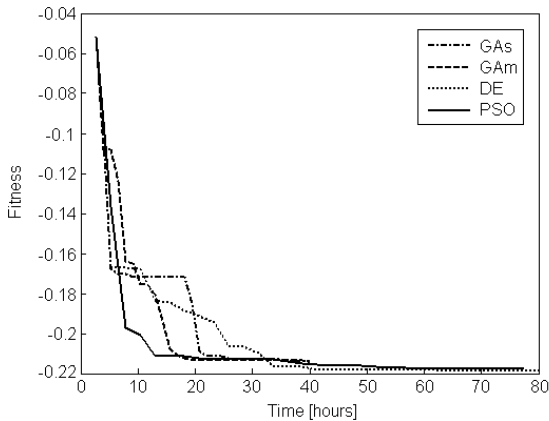


**Fig. 9.** Comparison of the selected methods of global evolutionary algorithms – design of a planar EBG unit cell.

	GAs	GAm	DE	PSO	
$D$ [mm]	15.00	14.50	15.02	14.80	
$P$ [mm]	11.86	12.30	11.98	11.96	
CST	$f_c$ [GHz]	5.53	5.50	5.47	5.53
MWS	BW [%]	20.93	21.61	20.96	21.90
HFSS	$f_c$ [GHz]	5.52	5.48	5.53	5.56
	BW [%]	19.47	20.18	20.98	21.09

**Tab. 1.** Optimization results – properties of the planar EBG unit cells designed by different global evolutionary algorithms.

modes along the irreducible Brillouin zone shown in Fig. 2b. Using CST MWS v. 2008 installed on a PC with the processor Intel Core Quad @ 2.66 GHz and 8 GB RAM, the average time for completing the dispersion characterization was estimated to 776 seconds. Because of the different setups of the techniques used, measuring the convergence velocity in time is reasonable. For an objective comparison of the methods, the initial population was composed from identical sets of individuals for all the algorithms, and the convergence curves were averaged over 3 realizations of the optimization (Fig. 9). Based on the results from Fig. 9, the fastest convergence exhibits the PSO algorithm, whereas differences in accuracy of the methods are negligible.

Please notice that the results presented here are only informative because of the low number of realizations (long computational time needed for the full-wave dispersion analysis). A more detailed study of this problem will be a part of future work.

### 3. Design of a Mushroom EBG

In the last section, the PSO algorithm is exploited in the design of a mushroom structure [9], [10] to obtain simultaneous EBG and AMC behavior at the required central frequency  $f_c = 5.5$  GHz. The period  $D$ , the patch size  $P$ , the via diameter  $d$ , the dielectric substrate height  $h$  and relative permittivity  $\epsilon_r$  are unit cell state variables (see Fig. 10).

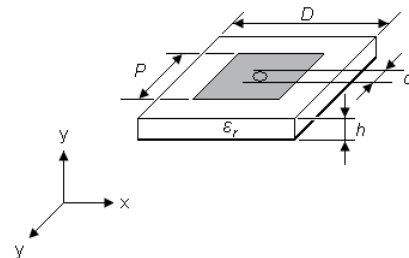


**Fig. 10.** The mushroom EBG unit cell.

The fitness function  $F$  is composed from partial fitness functions  $F_1$  and  $F_2$  considering both the band gap position and bandwidth and the frequency of zero reflection phase (the AMC point,  $f_{AMC}$ )

$$F = w_1 \cdot F_1^2 + w_2 \cdot F_2^2. \tag{4}$$

The partial fitness functions are defined as

$$F_1 = w_3 \cdot \left( \frac{f_{BG\_max} + f_{BG\_min}}{2} - f_c \right)^2 - w_4 \cdot \left( \frac{f_{BG\_max} - f_{BG\_min}}{f_c} \right) + 1 \tag{5}$$

and

$$F_2 = |f_{AMC} - f_c|. \tag{6}$$

In (4) and (5), values of weighting coefficients are set to  $w_1 = 0.75$ ,  $w_2 = 1$ ,  $w_3 = 1$  and  $w_4 = 0.25$ . Values of unit cell parameters are defined in the ranges included in Tab. 2.

Parameter	Range
$D$	<4.0 mm; 20.0 mm>
$P$	<0.50 $D$ ; 0.95 $D$ >
$d$	<0.2 mm; 2.0 mm>
$h$	<0.5 mm; 3.0 mm>
$\epsilon_r$	<1.0; 12.0>

Tab. 2. Mushroom EBG unit cell – parameters for optimization.

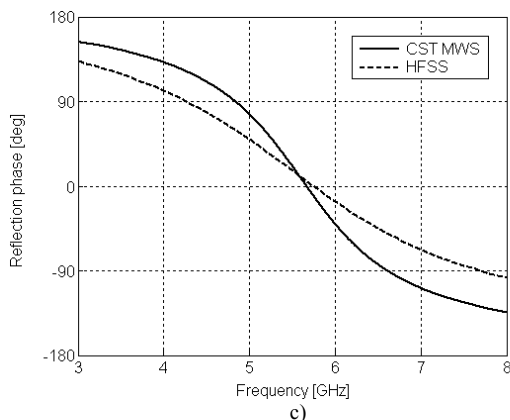
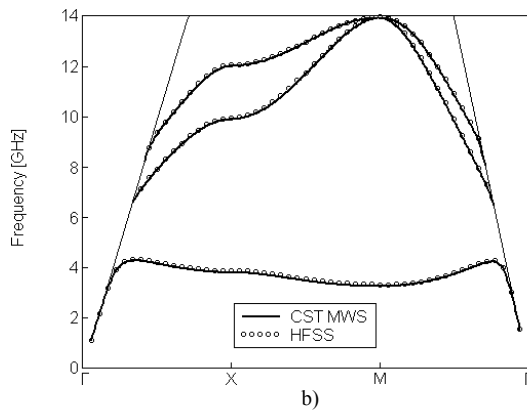
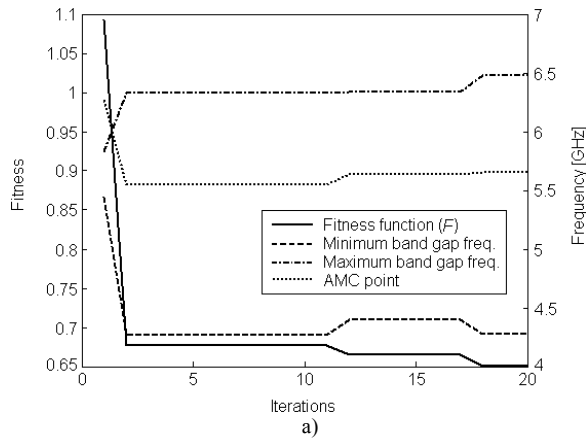


Fig. 11. Design of the mushroom structure by the PSO algorithm: evaluation of the fitness function, lower and upper limit of the band gap and frequency of the AMC point during 20 iterations (a), dispersion diagram (b) and reflection phase diagram (c) of the best individual.

In this case, the lowest band gap occurs between the first and the second dispersion curves (the TM surface wave suppression). The reflection phase was computed for the normal wave incidence by modeling a single unit cell only and using a de-embedded waveguide port with pairs of PEC (perfect electric conductor) and PMC (perfect magnetic conductor) walls.

$D$ [mm]	7.57	
$P$ [mm]	7.14	
$d$ [mm]	0.76	
$h$ [mm]	2.73	
$\epsilon_r$ [-]	2.78	
	CST MWS	HFSS
$f_{BG \text{ min}}$ [GHz]	4.28	4.33
$f_{BG \text{ max}}$ [GHz]	6.50	6.66
$f_{AMC}$ [GHz]	5.67	5.74

Tab. 3. Properties of the PSO designed mushroom unit cell.

The structure was optimized during 20 iteration steps. Clearly, the PSO algorithm gives good results already after two iterations (see Fig. 11a). The dispersion and the reflection phase diagram of the best individual (properties in Tab. 3) are depicted in Fig. 11b, c. The dispersion curves calculated by CST MWS and Ansoft HFSS are in an excellent agreement; HFSS shows a slightly flatter reflection phase curve implying a larger AMC bandwidth (reflection phase between -90 deg and +90 deg) as predicted by the CST MWS.

## 4. Conclusions

In the paper, the automated design of periodic structures with electromagnetic band gap properties was discussed. The developed method is based on full-wave calculation of the dispersion relation in CST Microwave Studio and an optimization by a global evolutionary algorithm implemented in Matlab. Four types of evolutionary algorithms – the genetic algorithm with single point or multi point crossover, the differential evolution and the particle swarm optimization – were tested and mutually compared in terms of convergence velocity and accuracy. In the last section, an example of the design of a conventional mushroom structure was described. The design was asked to obtain simultaneous EBG and AMC behavior in a certain frequency interval. Application of the presented technique in the design of more complex (e.g. multi-band) EBGs is straightforward.

## Acknowledgements

Research described in this contribution was financially supported by the Czech Science Foundation under the grants no. 102/07/0688 and 102/08/H018. The research is a part of the COST project IC0603.

## References

- [1] YUEHE, G., ESSELLE, K. P., BIRD, T. S. A high-gain low-profile EBG resonator antenna. In *Proc. of the Antennas and Propagation Society Int. Symp.* Honolulu (USA), 2007, p. 1301 – 1304.
- [2] KERN, D.J., WERNER, D.H., MONORCHIO, A., LANUZZA, L., WILHELM, M.J. The design synthesis of multiband artificial magnetic conductors using high impedance frequency selective surfaces. *IEEE Trans. Antennas Propag.*, 2005, vol. 53, no. 1, p. 8 – 17.
- [3] KOVÁCS, P., RAIDA, Z. Dispersion analysis of planar metallo-dielectric EBG structures in Ansoft HFSS. In *Proc. of the 17<sup>th</sup> Int. Conf. on Microwaves, Radar and Wireless Communications.* Wroclaw (Poland), 2008, p. 1 – 4.
- [4] KOVÁCS, P., RAIDA, Z., MARTÍNEZ-VÁZQUEZ, M. Parametric study of mushroom-like and planar periodic structures in terms of simultaneous AMC and EBG properties. *Radioengineering*, 2008, vol. 17, no. 4, p. 19 – 24.
- [5] JOHNSON, J. M., RAHMAT-SAMII, Y. Genetic algorithms in engineering electromagnetics. *IEEE Antennas and Propagation Magazine*, 1997, vol. 39, no. 4, p. 7 – 21.
- [6] ZELINKA, I. *Artificial Intelligence – Global Optimization.* Prague: BEN, 2002. (In Czech.)
- [7] *Differential evolution by Rainer Storn.* [Online] Available at: <http://www.icsi.berkeley.edu/~storn/code.html>
- [8] ROBINSON, J., RAHMAT-SAMII, Y. Particle swarm optimization in electromagnetics. *IEEE Trans. Antennas Propag.*, 2004, vol. 52, no. 2, p. 397 – 407.
- [9] SIEVENPIPER, D., ZHANG, L., BROAS, R. F. J., ALEXOPOULOS, N. G., YABLONOVITCH, E. High-impedance electromagnetic surfaces with a forbidden frequency band. *IEEE Trans. Microw. Theory Tech.*, 1999, vol. 47, no. 1, p. 2059 – 2074.
- [10] SIEVENPIPER, D. F. *High-Impedance Electromagnetic Surfaces.* Ph.D. Thesis, Los Angeles: Univ. of California (UCLA), 1999.

## About Authors ...

**Peter KOVÁCS** was born in Slovakia in 1984. He received the B.Sc. and M.Sc. degrees from the Brno University of Technology (BUT), Czech Republic, in 2005 and 2007, respectively. He is currently a Ph.D. student at the Dept. of Radio Electronics, BUT.

**Zbyněk RAIDA** - for biography see p. 110 in this issue.

# RADIOENGINEERING REVIEWERS I

April 2010, Volume 19, Number 1

- ARCE-DIEGO, J. L., University of Cantabria, Santander, Spain
- BALLING, P., Antenna Systems Consulting ApS, Denmark
- BONEFAČIĆ, D., University of Zagreb, Croatia
- COCHEROVÁ, E., Slovak University of Technology, Bratislava, Slovakia
- ČERMÁK, D., University of Pardubice, Jan Perner Transport Faculty, Czechia
- ČERNÝ, P., Czech Technical University in Prague, Czechia
- DJIGAN, V., R&D Center of Microelectronics, Russia
- DJORDJEVIC, I. B., University of Arizona, USA
- DOBEŠ, J., Czech Technical University in Prague, Czechia
- DRUTAROVSKÝ, M., Technical University of Košice, Slovakia
- FEDRA, Z., Brno Univ. of Technology, Czechia
- FONTAN, P. F., University of Vigo, Spain
- FRATTASI, S., Aalborg University, Denmark
- GALAJDA, P., Technical University of Košice, Slovakia
- GARRAMONE, G., German Aerospace Center, Germany
- GEORGIADIS, A., Centre Tecnologic de Telecomunicacions de Catalunya, Barcelona, Spain
- HANUS, S., Brno Univ. of Technology, Czechia
- HEŘMANSKÝ, H., The Johns Hopkins University, Maryland, USA
- HOFFMANN, K., Czech Technical University in Prague, Czechia
- HONZÁTKO, P., Academy of Sciences of the Czech Republic, Prague, Czechia
- HOSPODKA, J., Czech Technical University in Prague, Czechia
- HOZMAN, J., Czech Technical University in Prague, Czechia
- KASAL, M., Brno Univ. of Technology, Czechia
- KLÍMA, M., Czech Technical University in Prague, Czechia
- KOLÁŘ, R., Brno University of Technology, Czechia
- KOVÁCS, P., Brno Univ. of Technology, Czechia
- LAZAR, J., Academy of Sciences of the Czech Republic, Czechia
- LÁČÍK, J., Brno Univ. of Technology, Czechia